Electronic Supplementary Material (ESI) for Chemical Communications.

Supplementary Information

Control of Local Flexibility Towards *p*-Xylene Sieving in Hofmann-Type Porous Coordination Polymers

Mohana Shivanna,[a] Ken-ichi Otake,[a] Jia-Jia Zheng,[a,b] Shigeyoshi Sakaki,[b] and Susumu Kitagawa*[a]

[a]Institute for Integrated Cell-Material Sciences, Institute for Advanced Study, Kyoto University, Ushinomiya, Yoshida, Sakyo-ku, Kyoto 606-8501, Japan.

[b]Element Strategy Initiative for Catalyst and Batteries, Kyoto University, Goryo-Ohara 1-30, Nishikyo-ku, Kyoto 615-8245, Japan.

E-mail: kitagawa@icems.kyoto-u.ac.jp

Table of Contents

1.	Methods and Instrumentation	S03-4
2.	Physicochemical properties of xylene isomers	S05
3.	Powder X-ray diffraction (PXRD)	S06-8
4.	Thermogravimetric analysis (TGA)	S09-11
5.	Synchrotron PXRD	S12-13
6.	Vapor sorption at 308 K	S14
7.	Recyclability	S15-16
8.	^{1}H NMR spectral analysis	S17-24
9.	Analysis of ***px*** soaked CoPzNi	S25
10.	Coordination bond distances	S26-28
11.	Images of powder samples of three PCPs	S29
12.	Computational details	S30-35
13.	Supplementary references	S36

Methods and Instrumentation

All chemicals and solvents were purchased either from Tokyo Chemical Industries (TCI) or Sigma Aldrich and used without any further purification. Powder X-ray diffraction (PXRD) data were recorded on a Rigaku SmartLab X-ray diffractometer using Cu−K α radiation (λ = 1.54178 Å) by depositing powder on a glass substrate, from 2θ = 5° up to 40° with 0.02° increment. The TGA curves were obtained from a Rigaku TG 8120 analyzer (EVO2 TG/S-SL) using a heating rate of 5 °C min^{-1} under N_2 flow. Gas sorption of CO_2 and N_2 were carried out using BEL-mini or BEL-18 (Microtrac BEL Corp., Japan) gas adsorption instruments. Xylene vapor sorptions were measured by a BEL-max (Microtrac BEL Corp., Japan) gas adsorption instrument. Before all of gas and vapor sorption experiments, samples were reactivated at 120 °C under vacuum for overnight. The synchrotron PXRD data were collected using a synchrotron X-ray and multiple MYTHEN detectors of the BL02B2 beamline at Super Photon ring (SPring-8).

Vapor phase binary mixture selectivity: About 10 mg of activated samples of FePzNi and CoPzNi were placed in 2 ml vial. This vial again placed in a one neck 30 ml glass tube which containing 2 ml equimolar binary mixture of xylene isomers. To the glass tube, vacuum was applied to remove the moisture from empty space and then placed at 35 °C. About one week later, the sample vial was taken out from the glass tube, and $CDCl_3$ was added immediately. After soaking for 1 hr and sonication and centrifuge, a saturated solution was used to measure ^1H NMR spectra on Brucker models Ultrashild 500 Plus NMR spectrometer, where chemical shifts (δ in ppm) were determined with a residual proton of the solvent as standard. For separation of a binary mixture of components *i* and *j*, the adsorption selectivity (S_{ij}) was calculated using the following equation:

$$S_{ij} = x_i/x_j$$

, where x_i and x_j denote the integrated areas of the each components in the NMR spectra.
In this work, the methyl groups of xylene isomers were considered.

Synthesis of Hofmann type PCPs

Preparation of [Fe(Pz)[Ni(CN)$_4$]: Iron(II)chloride tetrahydrate ($FeCl_2.4H_2O$ of 0.002 M, 397 mg) and potassium tetracyano nickelate(II) (K_2NiCN_4 of 0.002 M, 481.5 mg) in ethanol/water (1:1, 20ml each) was added simultaneously into stirring solution of pyrazine (0.002 M, 160 mg) taken in ethanol/water (1:1, 20ml). After overnight stirring at room temperature, a fine orange yellow powder was isolated and washed with ethanol/water mixture before use of further characterization. The obtained product from this reaction was 550 mg and calculated yield was 79%.

Preparation of [Co(Pz)[Ni(CN)$_4$]: Cobalt(II)chloride hexahydrate ($CoCl_2.6H_2O$ of 0.002 M, 474 mg) and potassium tetracyano nickelate(II) (K_2NiCN_4 of 0.002 M, 481.5 mg) in ethanol/water (1:1, 20ml each) was added simultaneously into stirring solution of pyrazine (0.002 M, 160 mg) taken in ethanol/water (1:1, 20ml). After overnight stirring at room temperature a light pink color powder was isolated and washed with ethanol/water mixture before the use of further characterization. The obtained product from this reaction was 500 mg and the calculated yield was 72%.

Preparation of [Ni(Pz)[Ni(CN)$_4$]: Nickel(II)chloride hexahydrate ($NiCl_2.6H_2O$ of 0.002 M, 474 mg) and potassium tetracyano nickelate(II) (K_2NiCN_4 of 0.002 M, 481.5 mg) in ethanol/water (1:1, 20ml each) was added simultaneously into stirring solution of pyrazine (0.002 M, 160 mg) taken in ethanol/water (1:1, 20ml). After overnight stirring at room temperature a slate blue color powder was isolated and washed with ethanol/water mixture before use of further characterization. The obtained product from this reaction was 450 mg and the calculated yield 65%.

	para-xylene	*meta*-xylene	*ortho*-xylene
		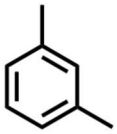	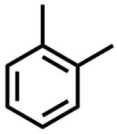
Kinetic diameter(Å)	6.7	7.1	7.4
Boiling point(K)	411.5	412.3	417.6
Freezing point(K)	286.4	222.5	248.0
Dipole moment(D)	0	0.36(liquid)	0.62(gas)
Polarizability(cm^3)	13.7	14.2	14.9
Density at 198K (gcm^{-3})	0.858	0.861	0.876

Table S1: Representation of physicochemical properties of three xylene isomers.[1]

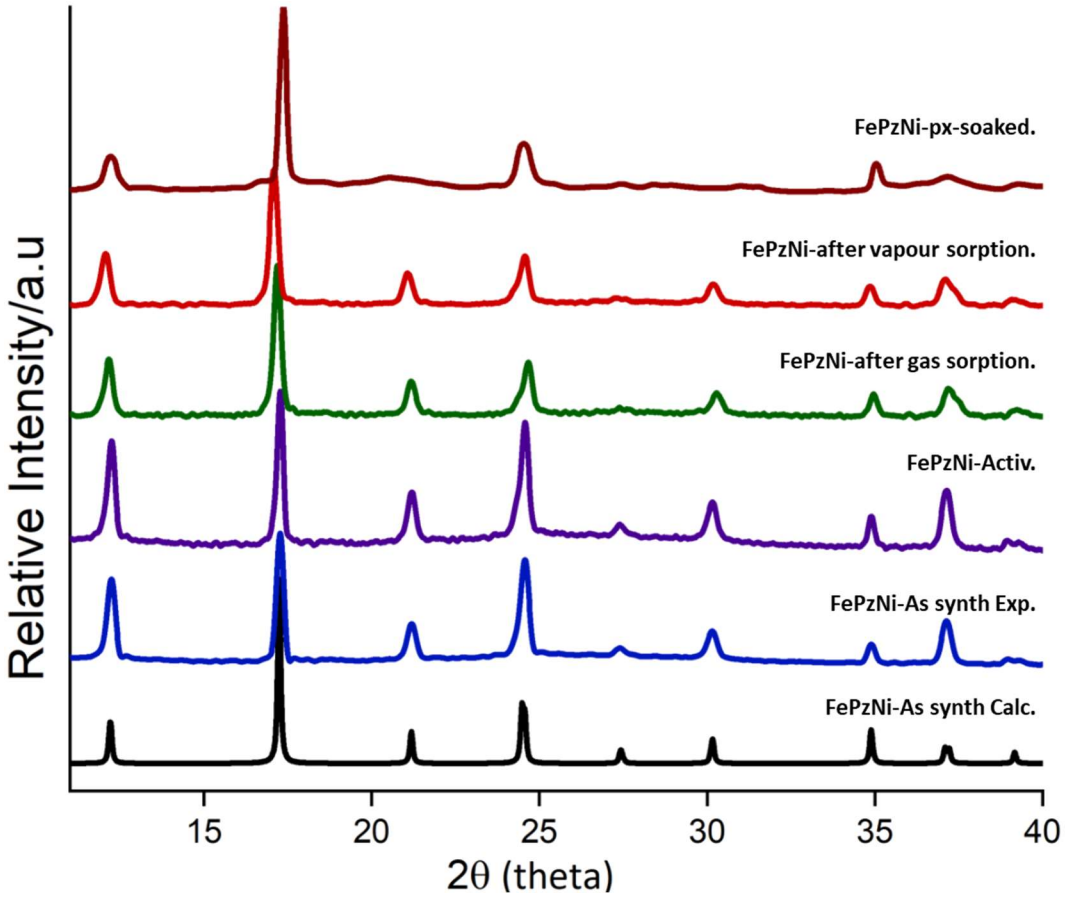

Figure S1: PXRD comparison of as synthesized, activated, after gas sorption, after vapor sorption and after ***px-*** soaked experiments obtained for FePzNi.

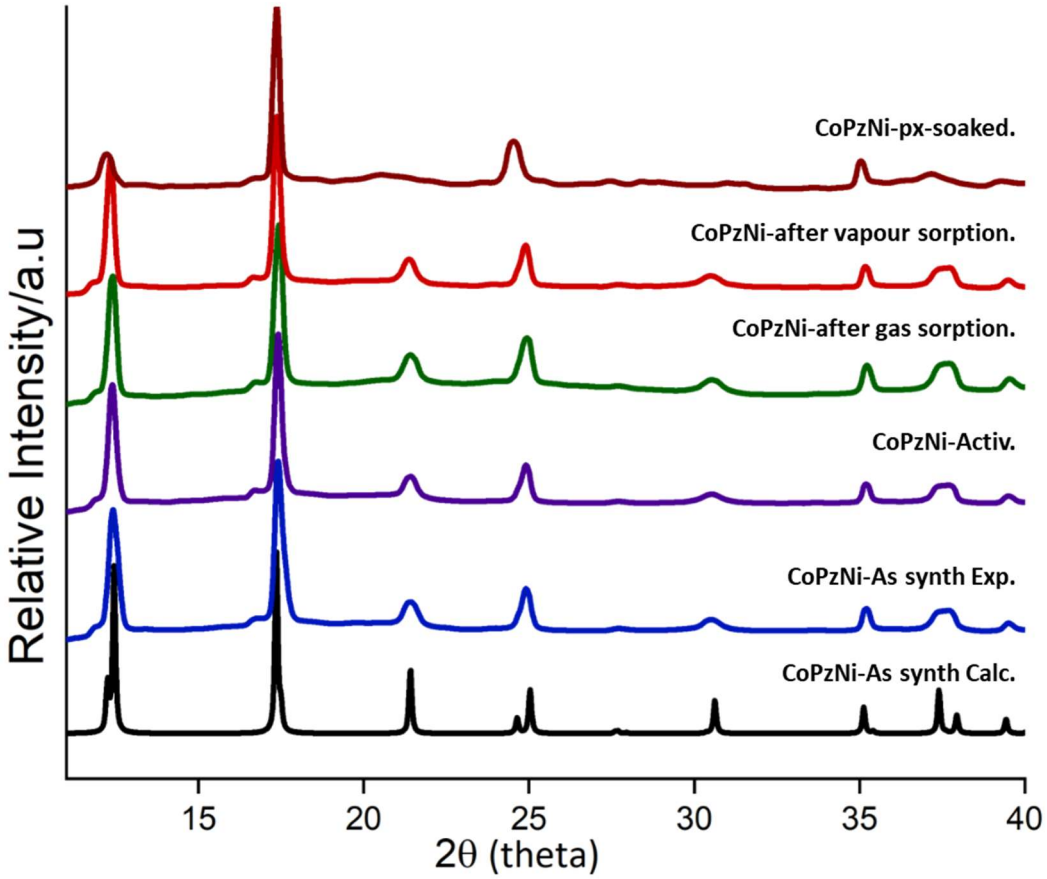

Figure S2: PXRD comparison of as synthesized, activated, after gas sorption, after vapor sorption and ***px***-soaked experiments obtained for CoPzNi.

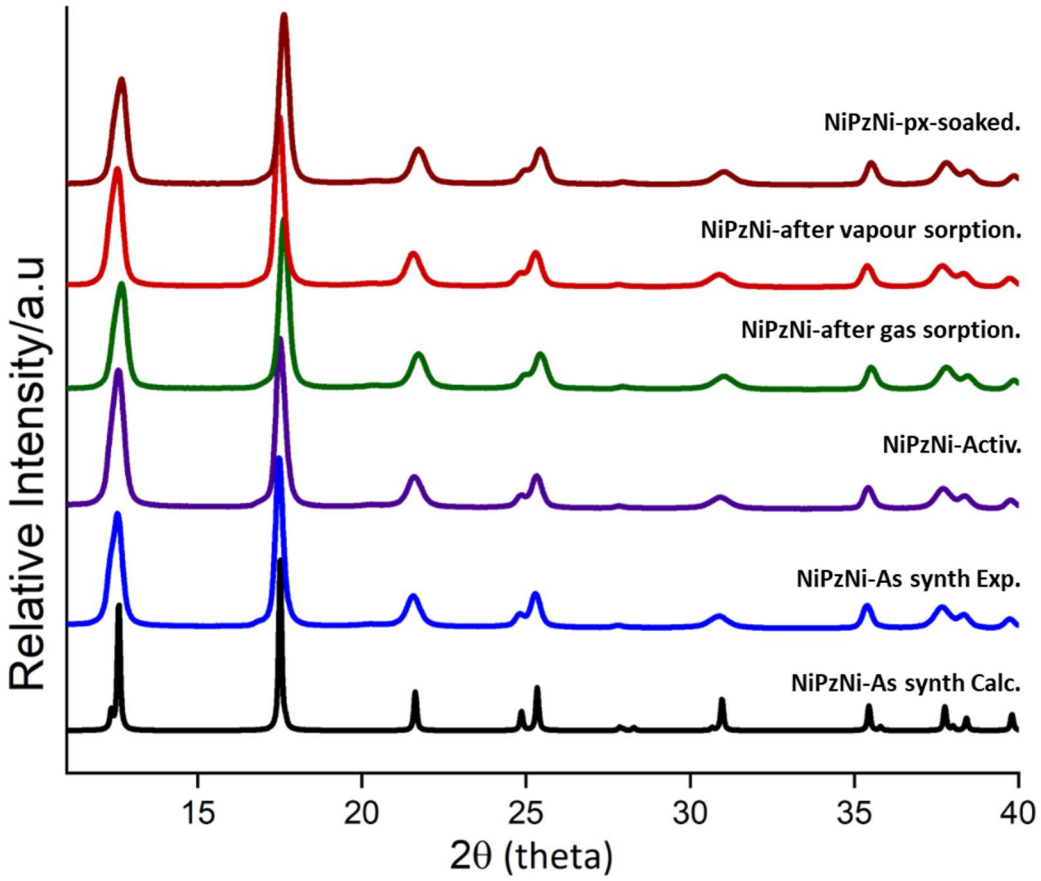

Figure S3: PXRD comparison of as synthesized, activated, after gas sorption and vapor sorption experiments obtained for NiPzNi.

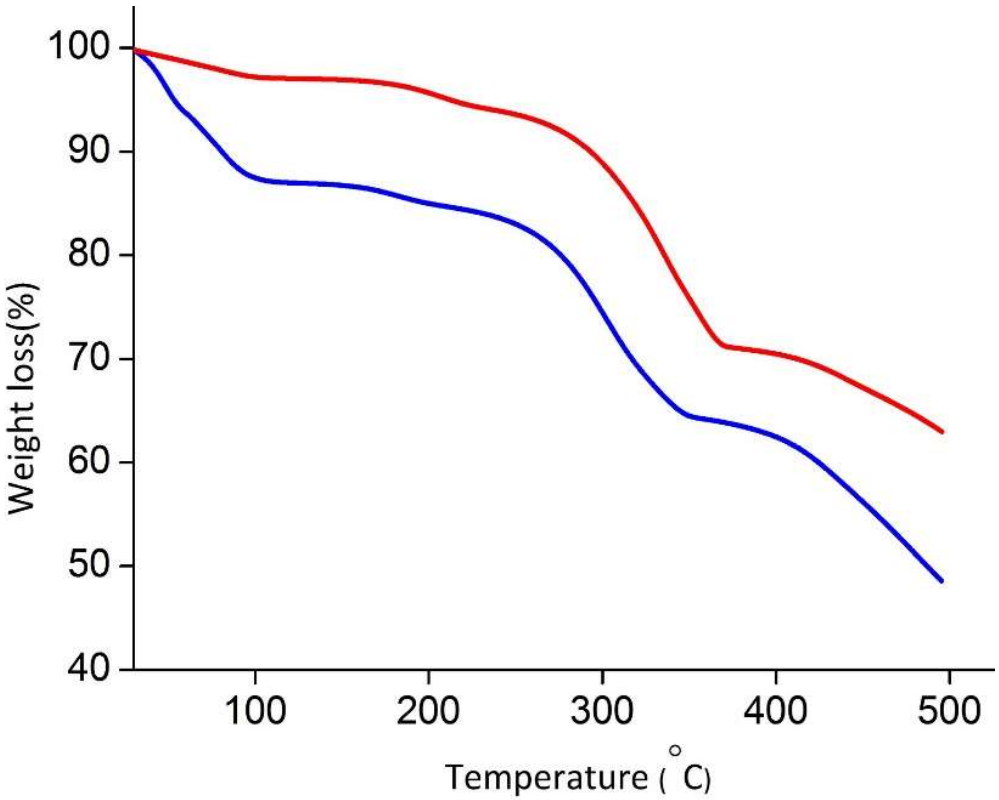

Figure S4: Thermogravimetric measurements of as synthesized (blue) and activated (red) phase of FePzNi. The observed weight loss ~13 % were attributed to the loss of 2.5 H_2O molecules per formula unit and the thermal stability was found up to ~250 °C, which is lower than both CoPzNi and NiPzNi. This is mainly attributed to longer bond distances between the Fe and the N atom of the pyrazine ($D_{Fe\cdots N}$ = 2.212 Å) and N atom of the cyanide ($D_{Fe\cdots N}$ = 2.117 Å). The square planar metal center of Ni and C atom of the cyanide distance was $D_{Ni\cdots C}$ = 1.864 Å (Figure S20).

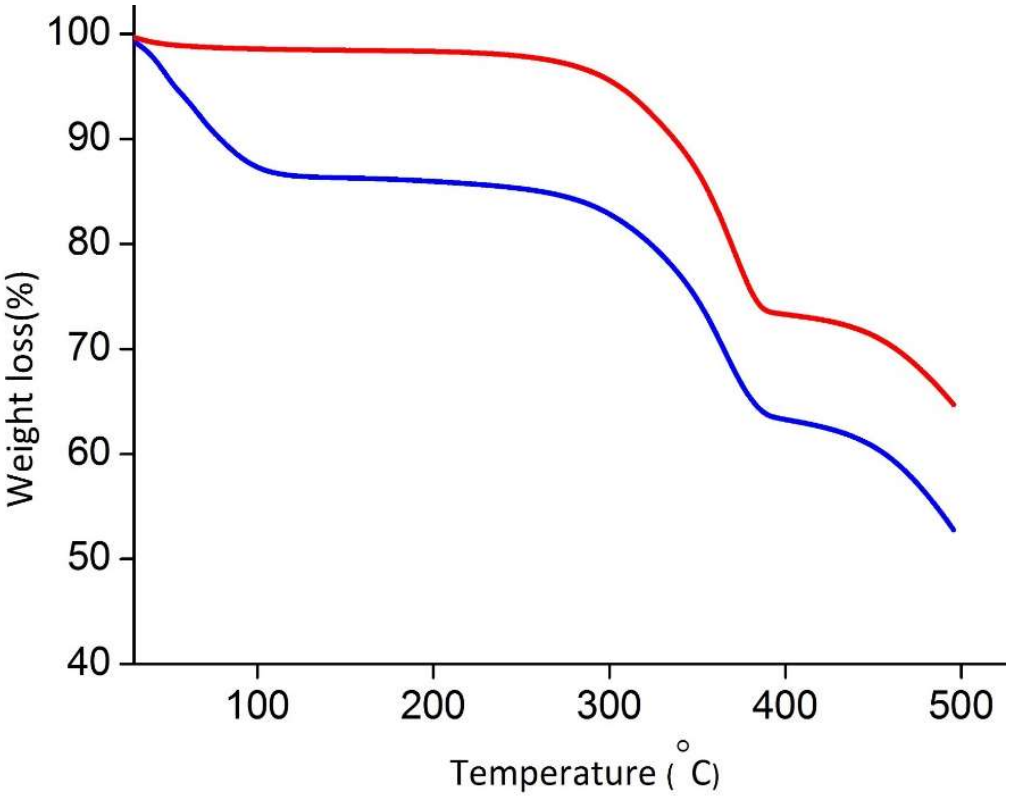

Figure S5: Thermogravimetric measurements of as synthesized (blue) and activated (red) phase of CoPzNi. The observed weight loss ~13.3 % were attributed to the loss of 2.5 H_2O molecules per formula unit and the thermal stability of CoPzNi was found up to ~280 °C which is slightly higher than FePzNi and lower than NiPzNi. This is due to reduce in bond distances between the octahedral center of Co and the N atom of the pyrazine ($D_{Co\cdots N}$ = 2.167 Å) and N atom of the cyanide ($D_{Co\cdots N}$ = 2.089 Å). Further, square planar center held with shorter distance between Ni and C atom of the cyanide was $D_{Ni\cdots C}$ = 1.858 Å (Figure S22).

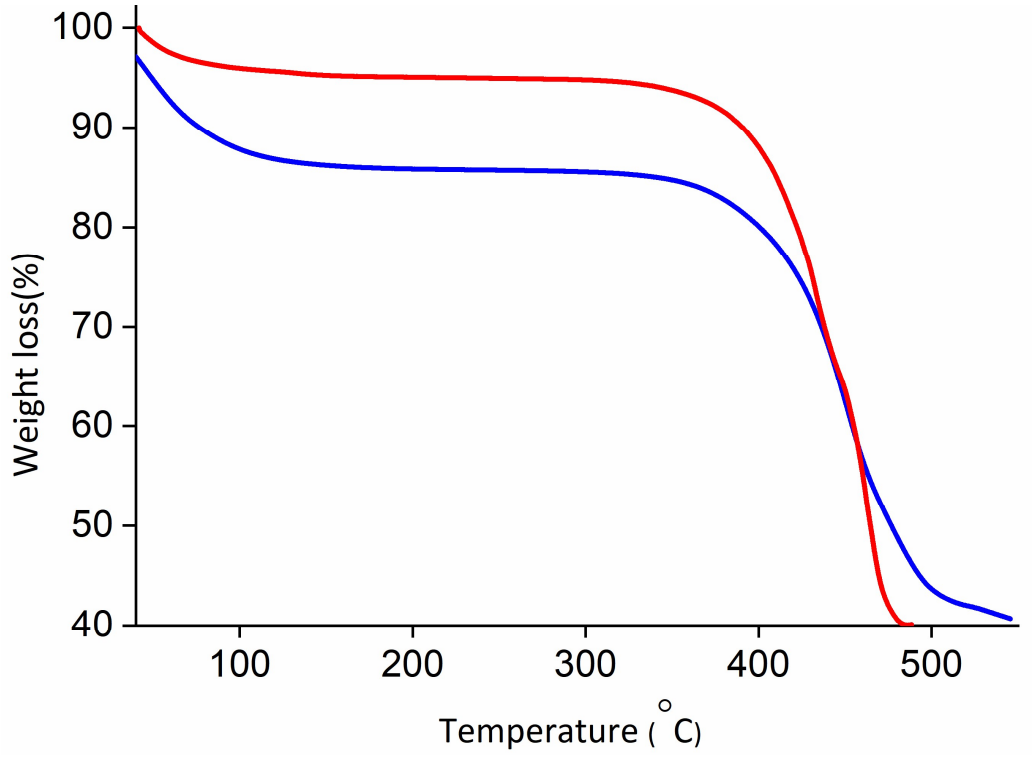

Figure S6: Thermogravimetric measurements of as synthesized (blue) and activated (red) phase of NiPzNi. The observed weight loss ~14 % were attributed to the loss of 2.5 H_2O molecules per formula unit and the thermal stability of NiPzNi was found up to ~350 °C which is higher than both FePzNi and CoPzNi. This increase in stability due to much shorter bond distances in case of NiPzNi for example, distance between the octahedral metal center of Ni and the N atom of the pyrazine was $D_{Ni\cdots N}$ = 2.037 Å and square planar center of Ni and the C atom of the cyanide was $D_{Ni\cdots C}$ = 1.825 Å (Figure S21).

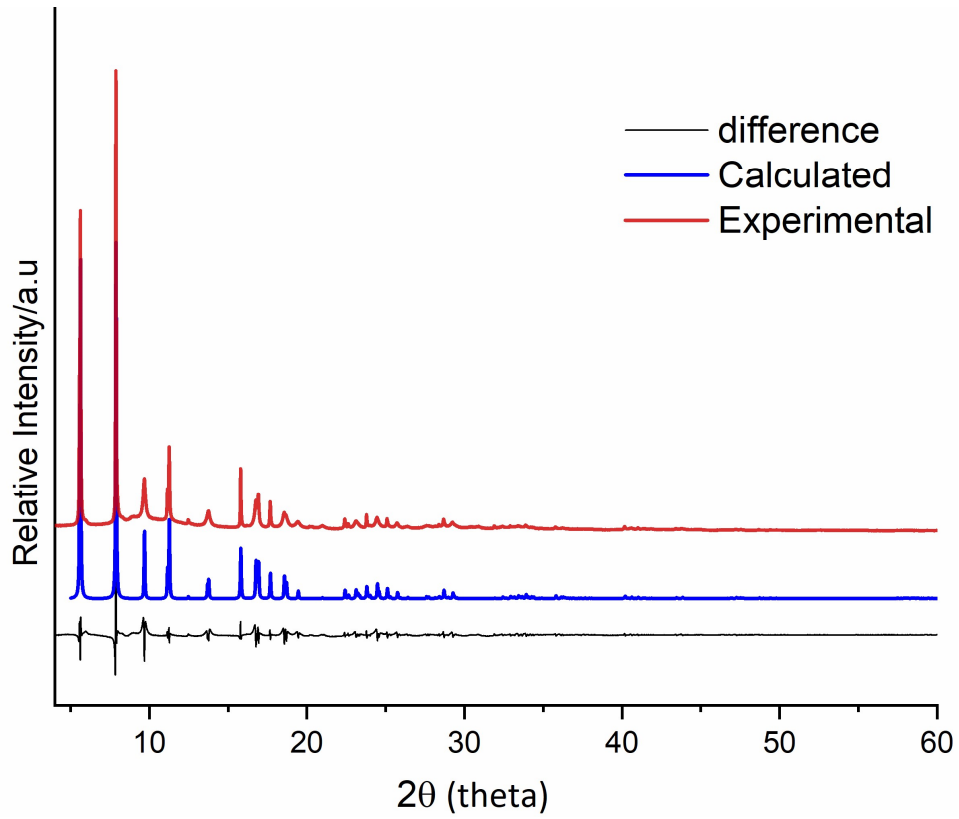

Figure S7: Synchrotron PXRD collected for activated CoPzNi (red) using wavelength (0.700Å), calculated PXRD (blue) obtained after refinement of cell parameters and the difference in diffraction pattern represented in black. Refinement was carried out using space group p4/mmm and obtained unit cell, a =7.199 (97), c =7.128 (15) and v =369.504 (15), which slightly smaller than FePzNi. The refinement of the activated CoPzNi confirmed that no phase change was observed, and the unit cell matched with previously reported crystal structure.

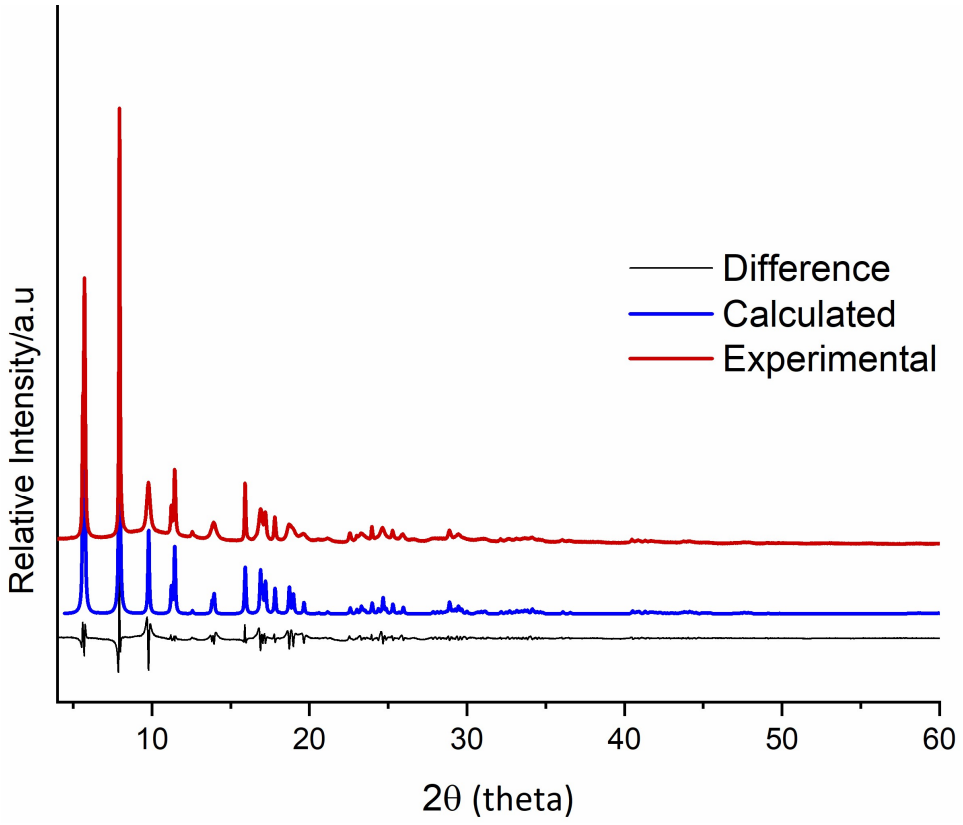

Figure S8: Synchrotron PXRD collected for activated NiPzNi (red) using wavelength (0.700Å), calculated PXRD (blue) obtained after refinement of cell parameters and the difference in diffraction pattern represented in black. Refinement was carried out using space group p4/m and obtained unit cell, a =7.146 (15), c =7.016 (24) and v =359.39 (20), which same as NiPzNi as synthesized form. The refinement of the activated NiPzNi confirmed that no phase change was observed, and the unit cell parameters matched with previously reported crystal structure.

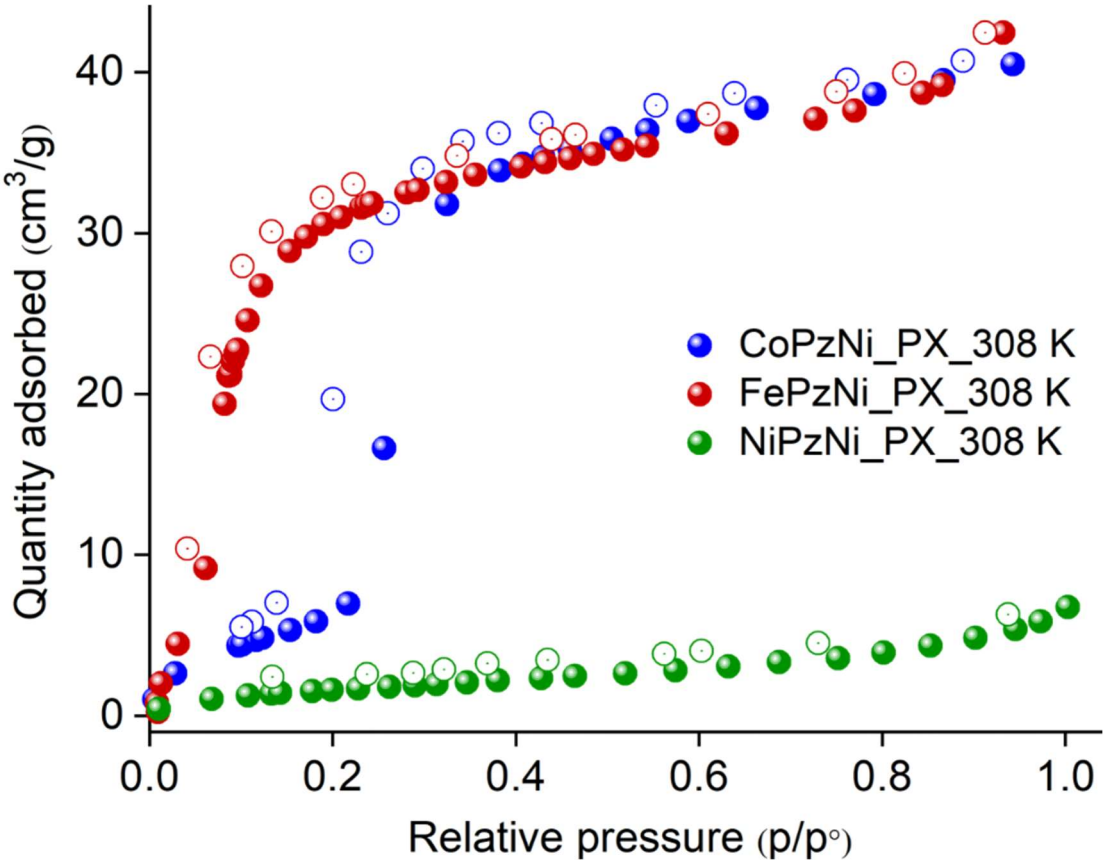

Figure S9: Vapor sorption of ***px*** isomer at 308 K for FePzNi (red), CoPzNi (blue) and NiPzNi (green).

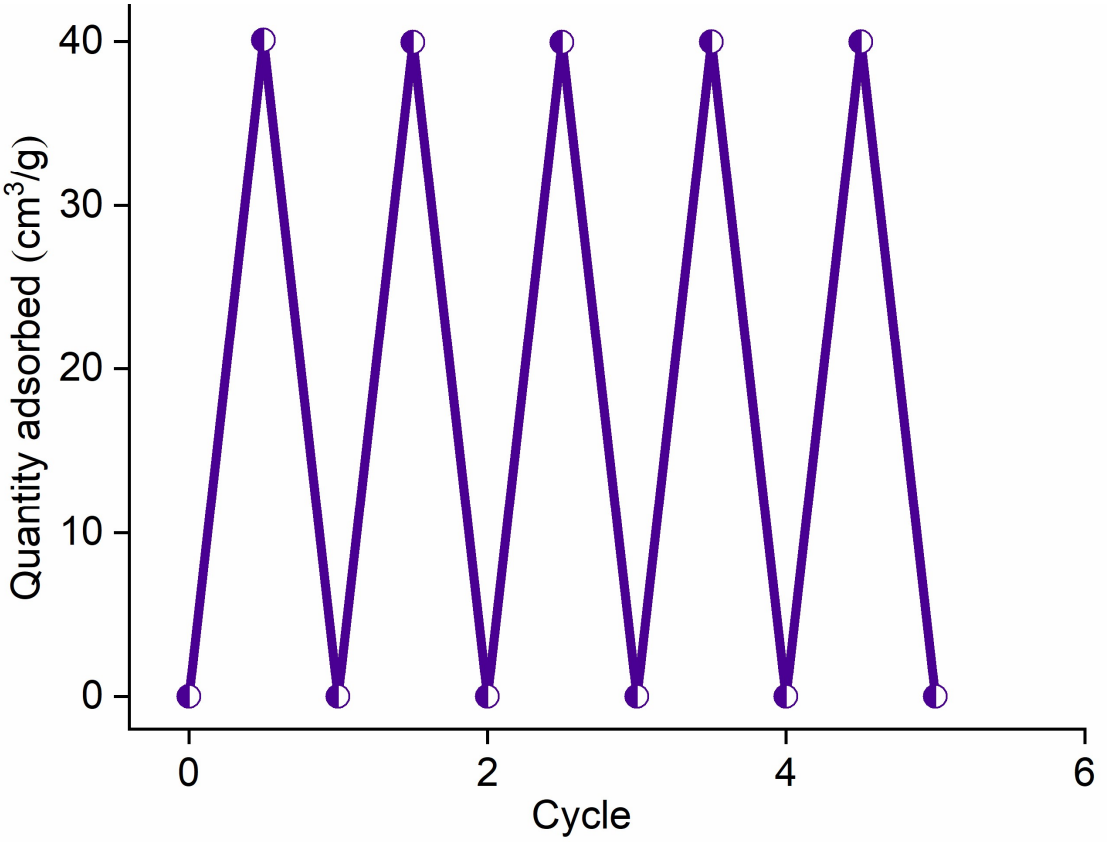

Figure S10: Recyclability of ***px*** isomer sorption measured up to 5cycles at 298 K for FePzNi.

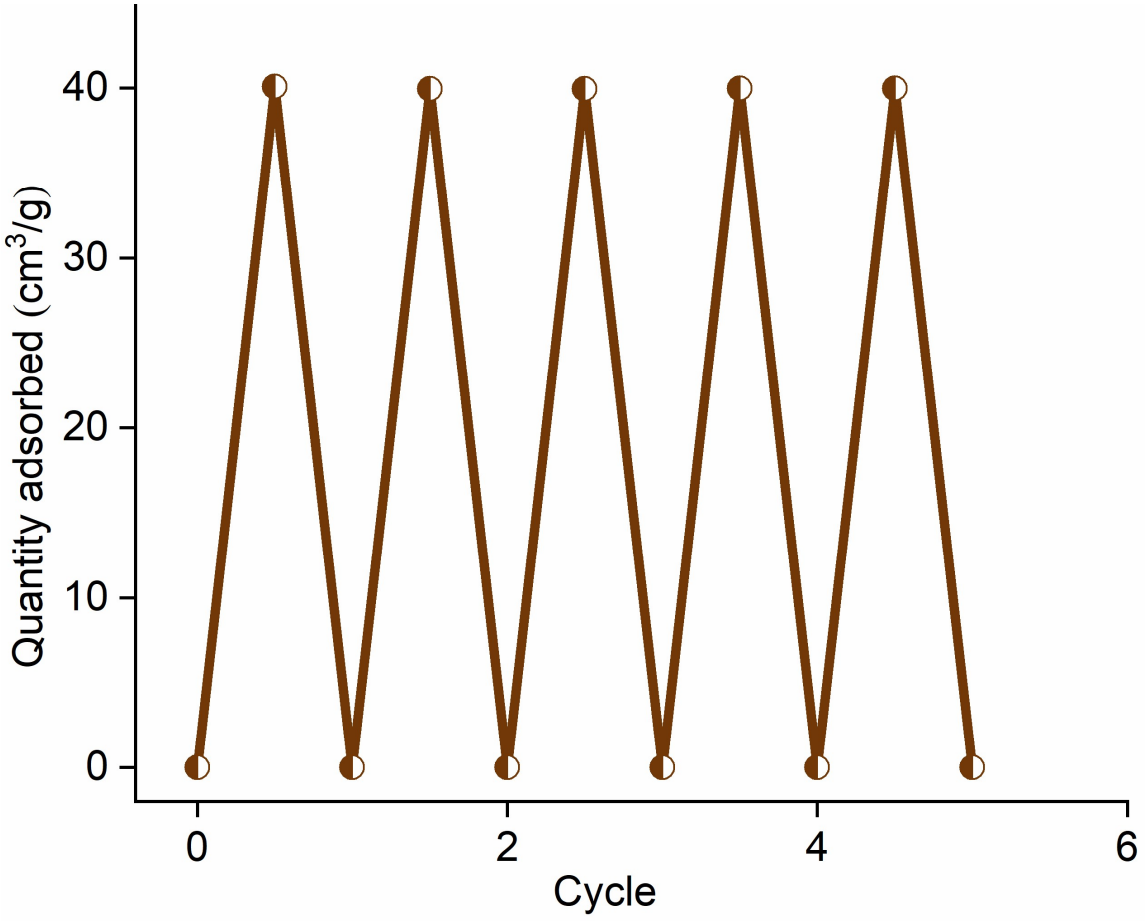

Figure S11: Recyclability of ***px*** isomer sorption measured up to 5cycles at 298 K for CoPzNi.

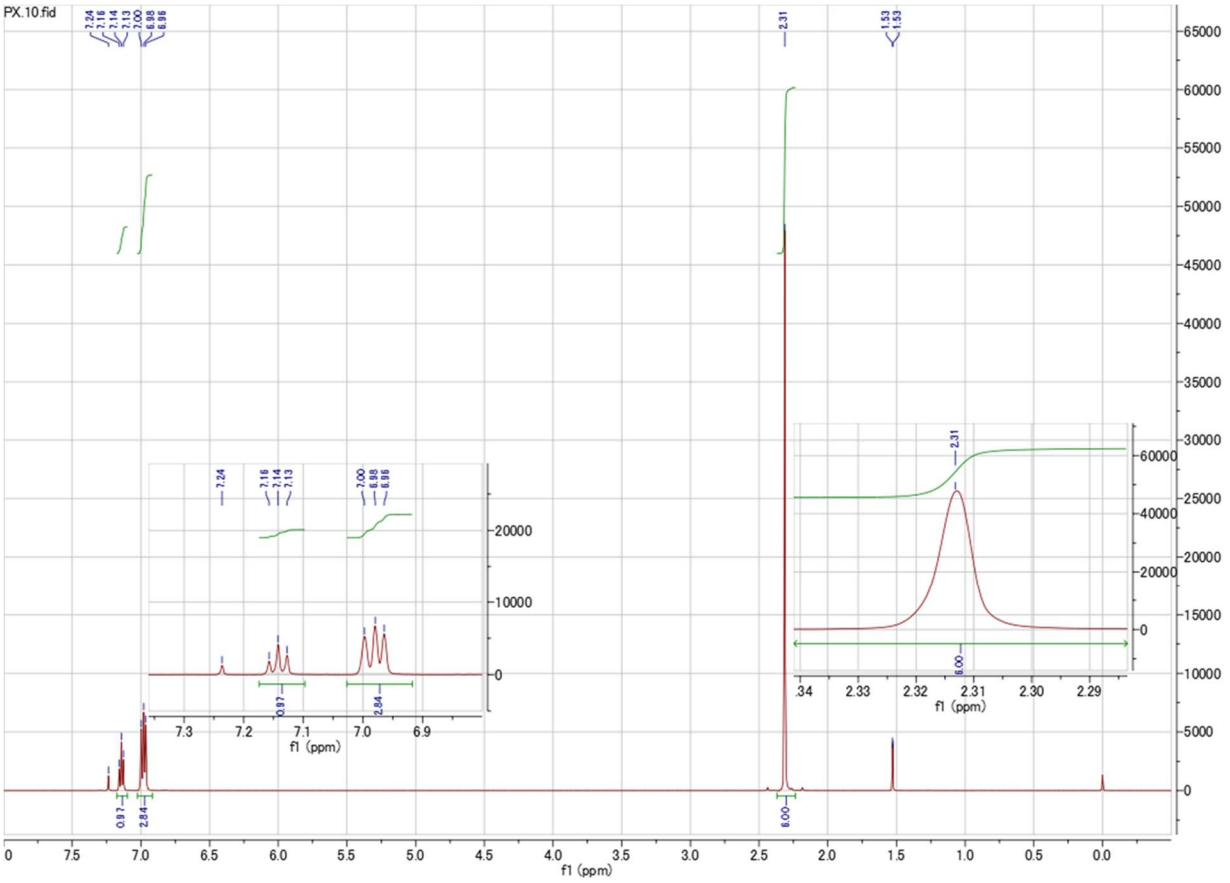

Figure S12: ^{1}H NMR spectra of pure ***px*** isomer measured using $CDCl_3$.

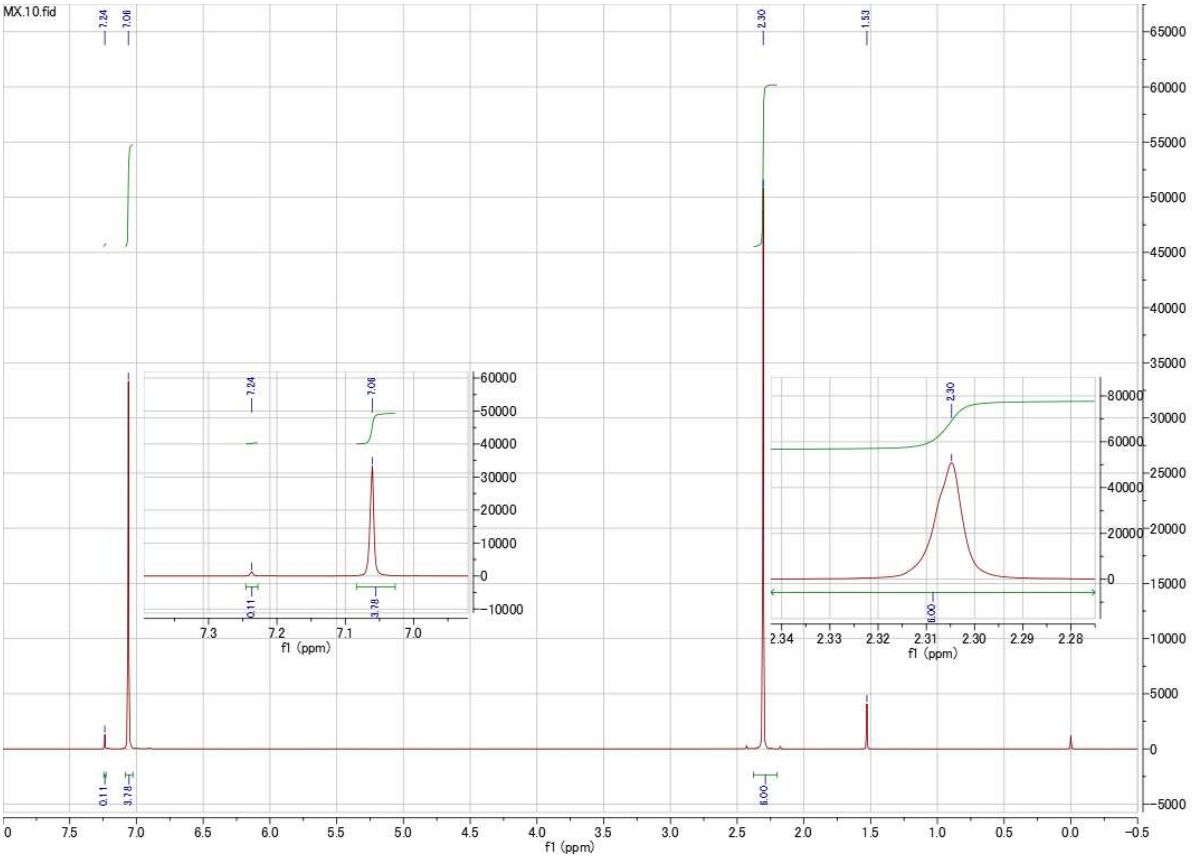

Figure S13: ^{1}H NMR spectra of pure ***mx*** isomer measured using $CDCl_3$.

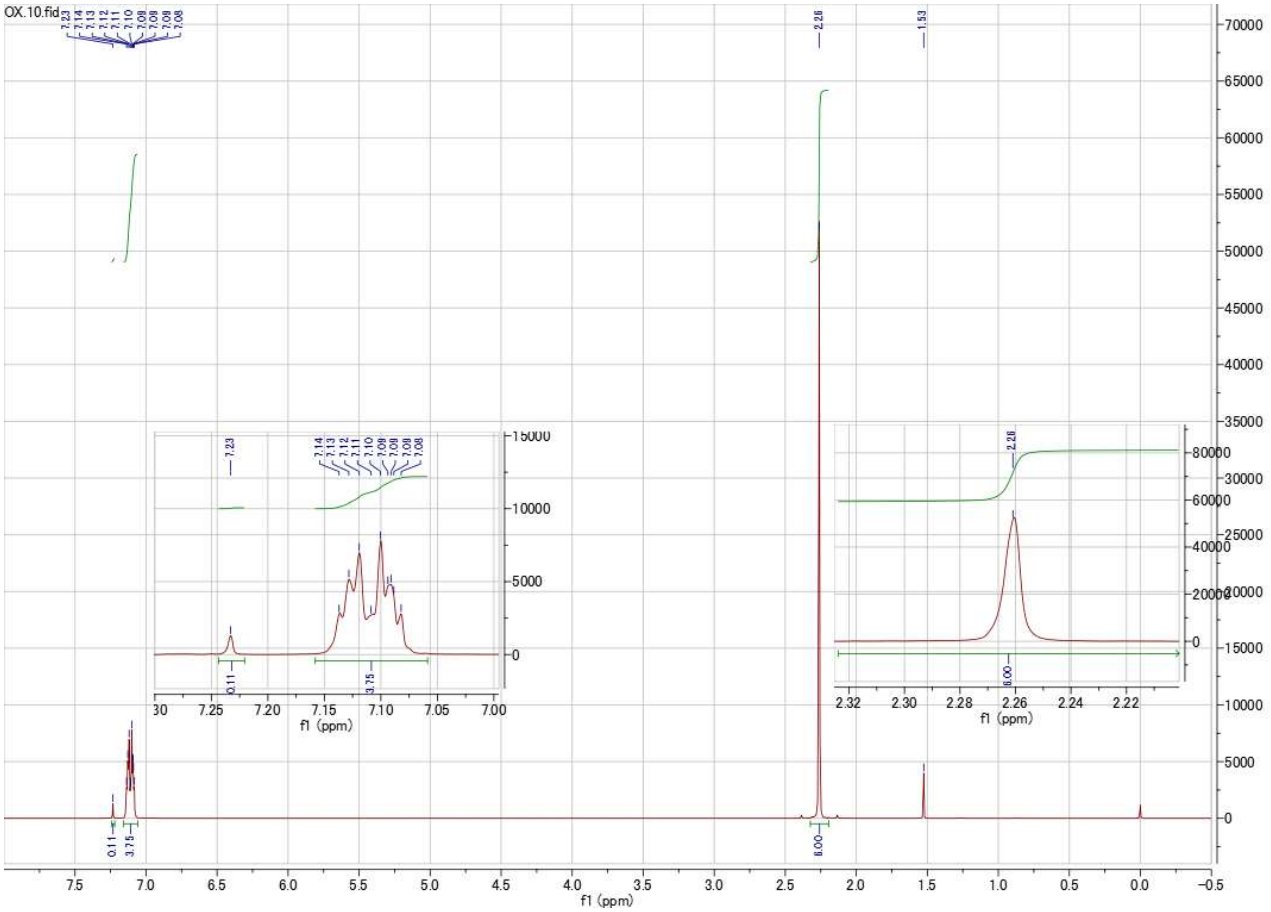

Figure S14: ^{1}H NMR spectra of pure ***ox*** isomer measured using $CDCl_3$.

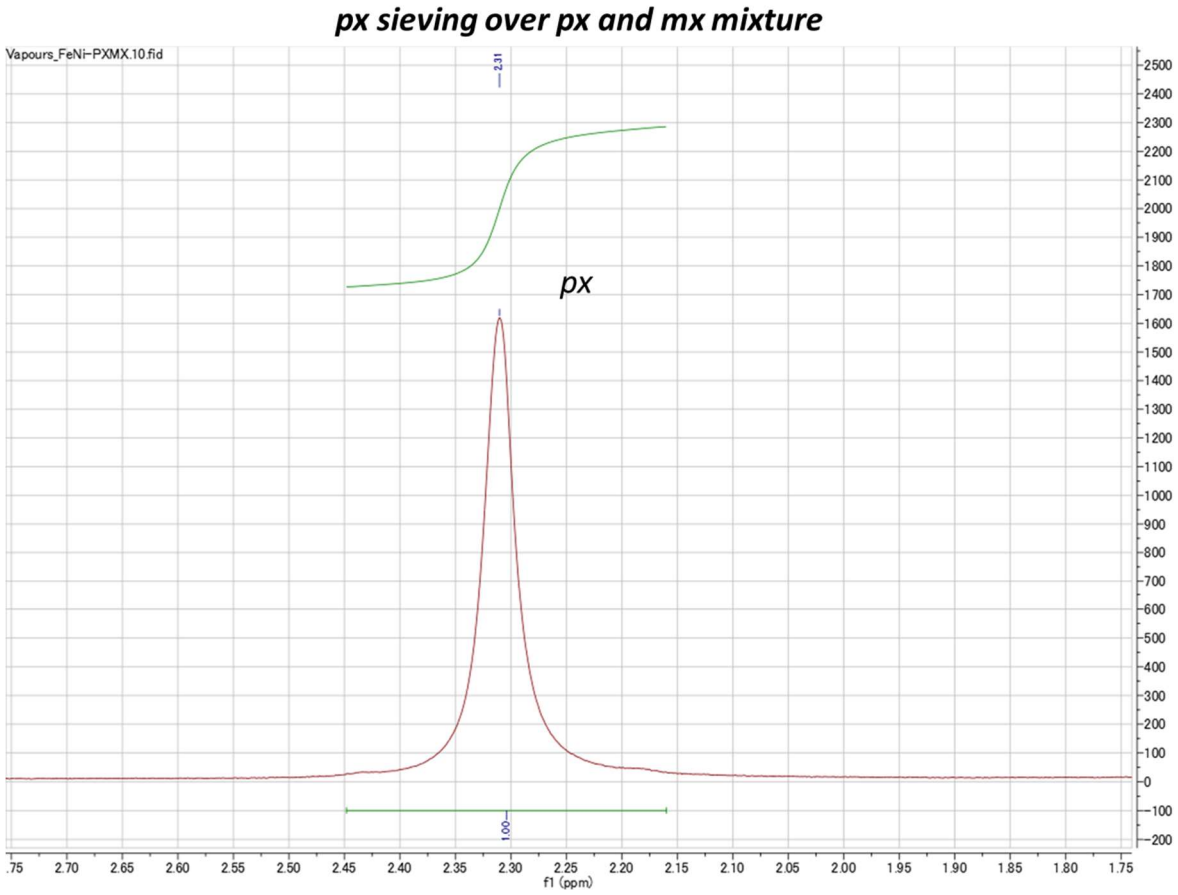

Figure S15: Magnified ^{1}H NMR spectra measured using the $CDCl_3$ extract of ***px/mx*** mixture from vapour phase experiment with respect to FePzNi.

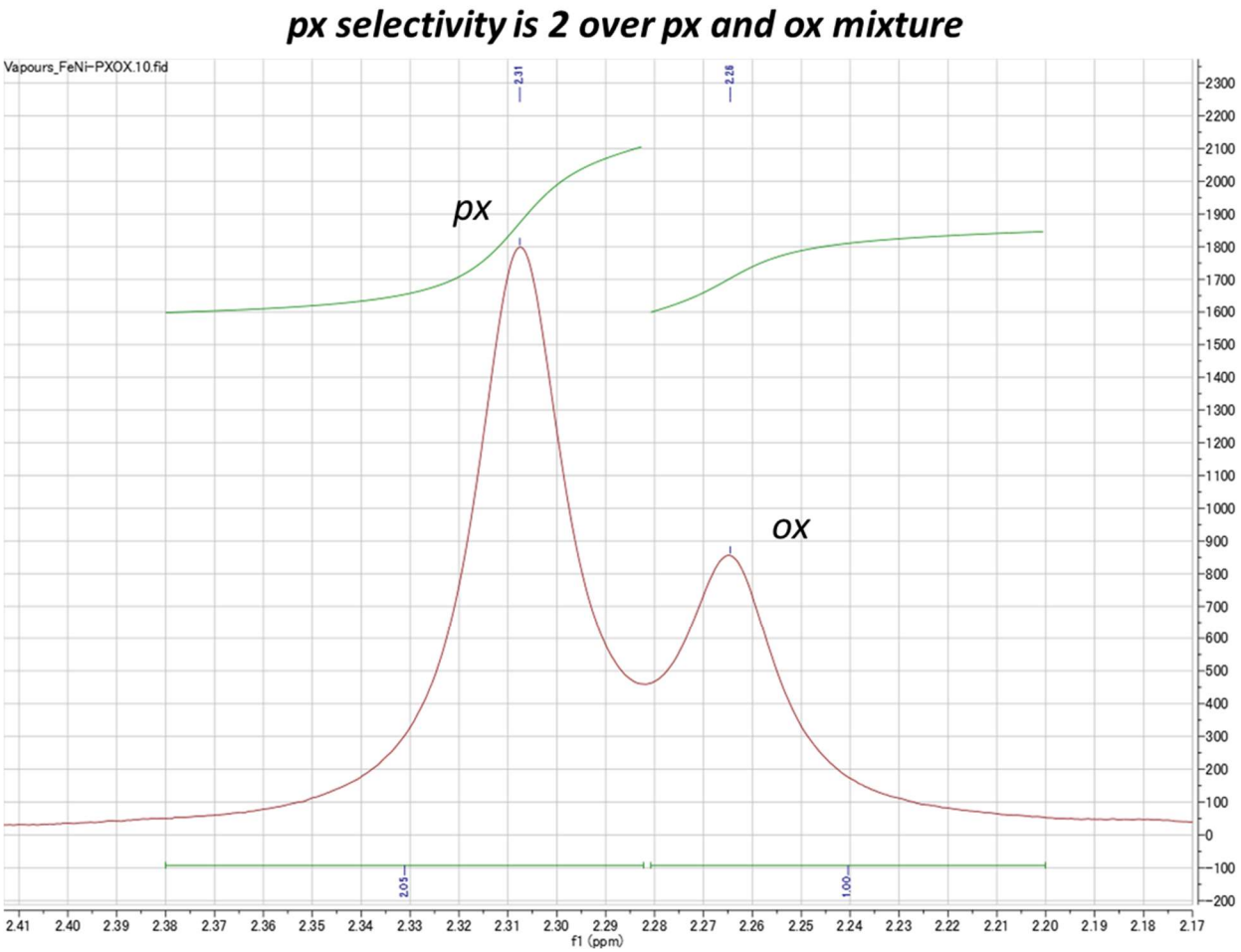

Figure S16: Magnified ^{1}H NMR spectra measured using the $CDCl_3$ extract of ***px/ox*** mixture from vapor phase experiment with respect to FePzNi.

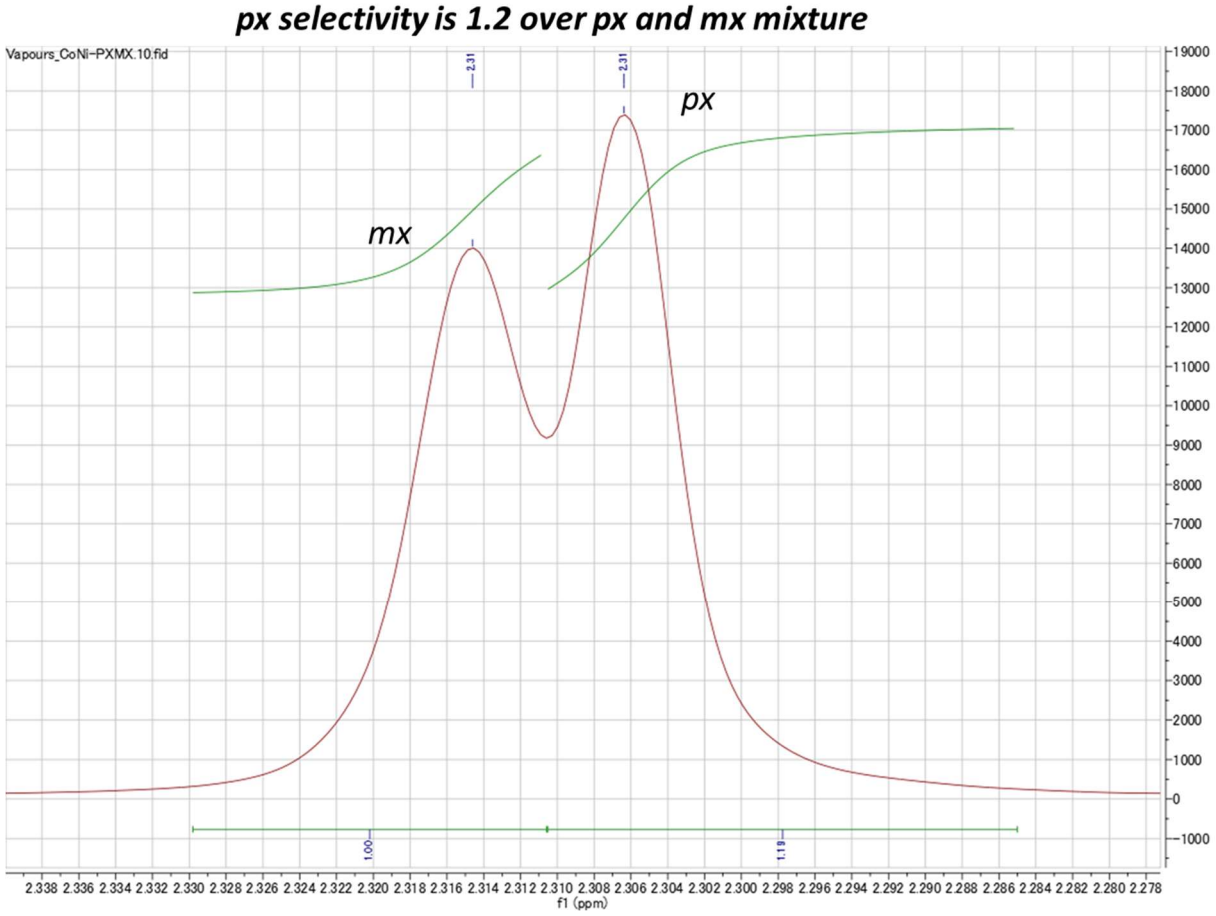

Figure S17: Magnified ^{1}H NMR spectra measured using the $CDCl_3$ extract of ***px/mx*** mixture from vapor phase experiment with respect to CoPzNi.

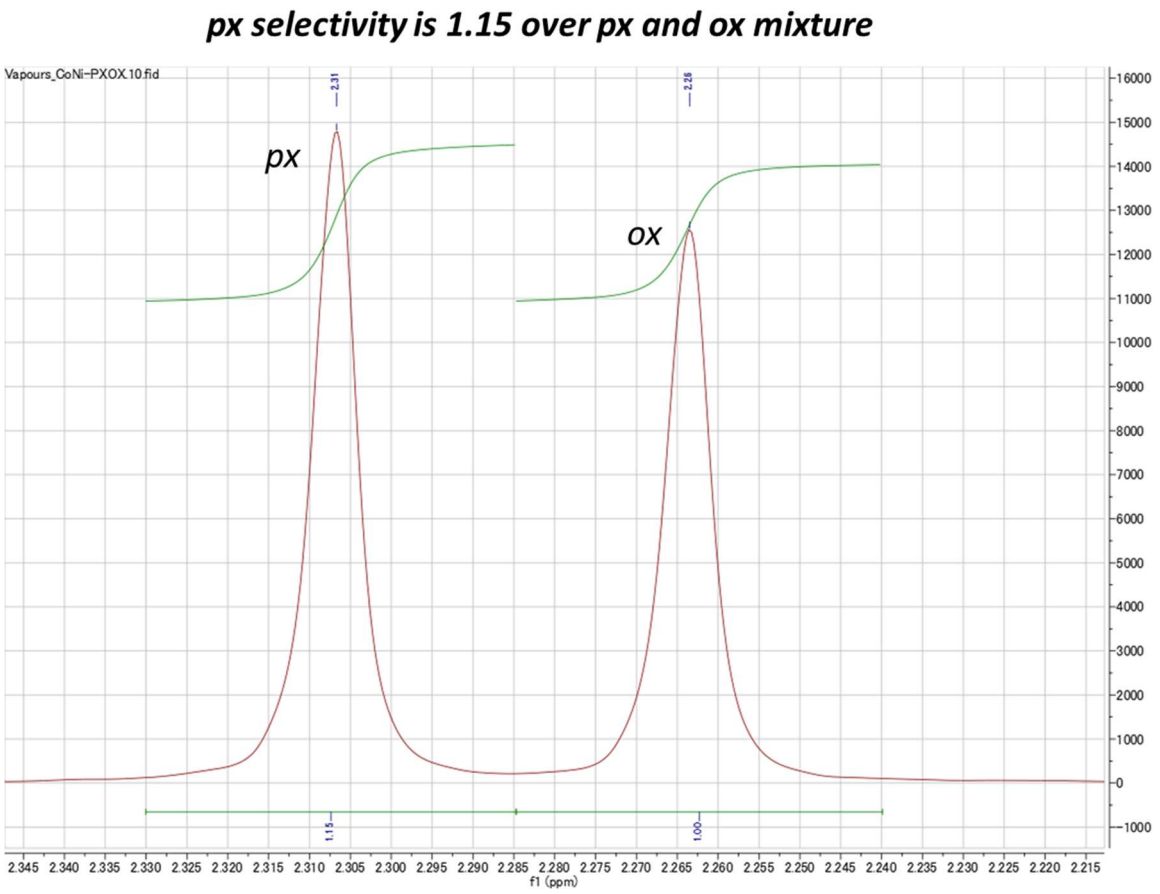

Figure S18: Magnified ^{1}H NMR spectra measured using the $CDCl_3$ extract of ***px/ox*** mixture from vapor phase experiment with respect to CoPzNi.

Adsorbent	*px/mx*	*px/ox*
Cu_3(BTC)	0.9	1.4
Mil-53(Al)ht	0.8	0.3
MIL-47	2.9	0.7
FePzNi	***px*-selective**	2
CoPzNi	1.2	1.15

Table S2: Vapor phase binary mixture (***px/mx*** and ***px/ox)*** selectivity comparison with the reported work.[2]

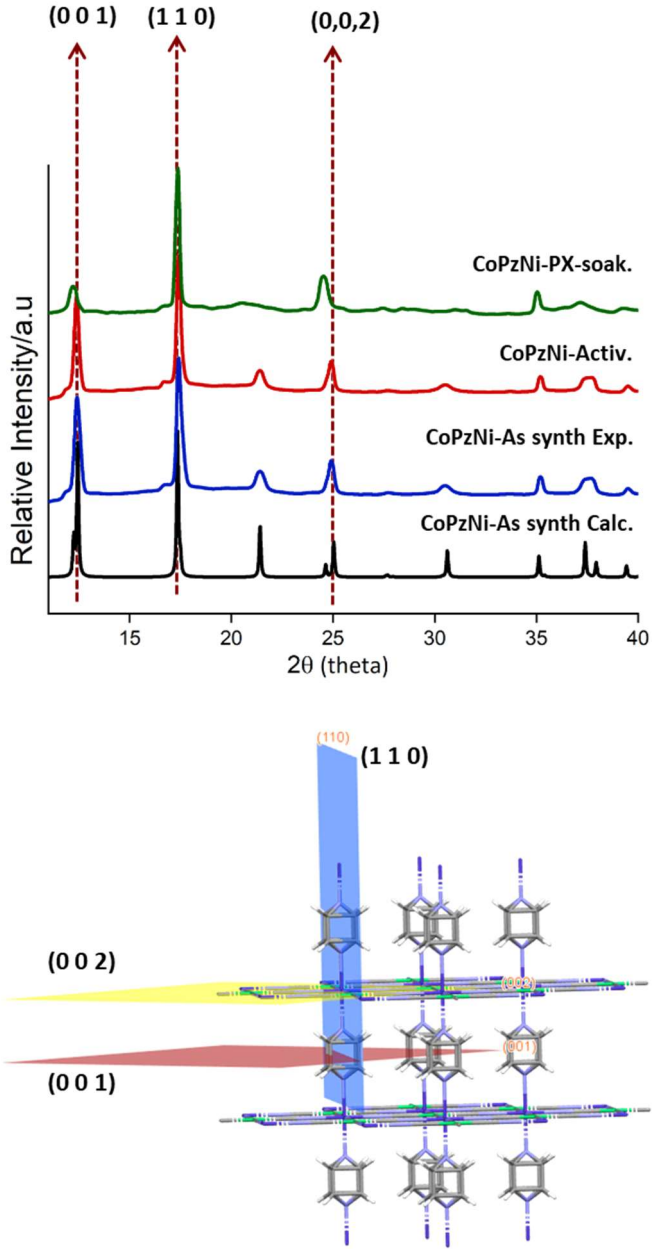

Figure S19: Representation of shift in peaks after soaking CoPzNi activated phase in ***px***.

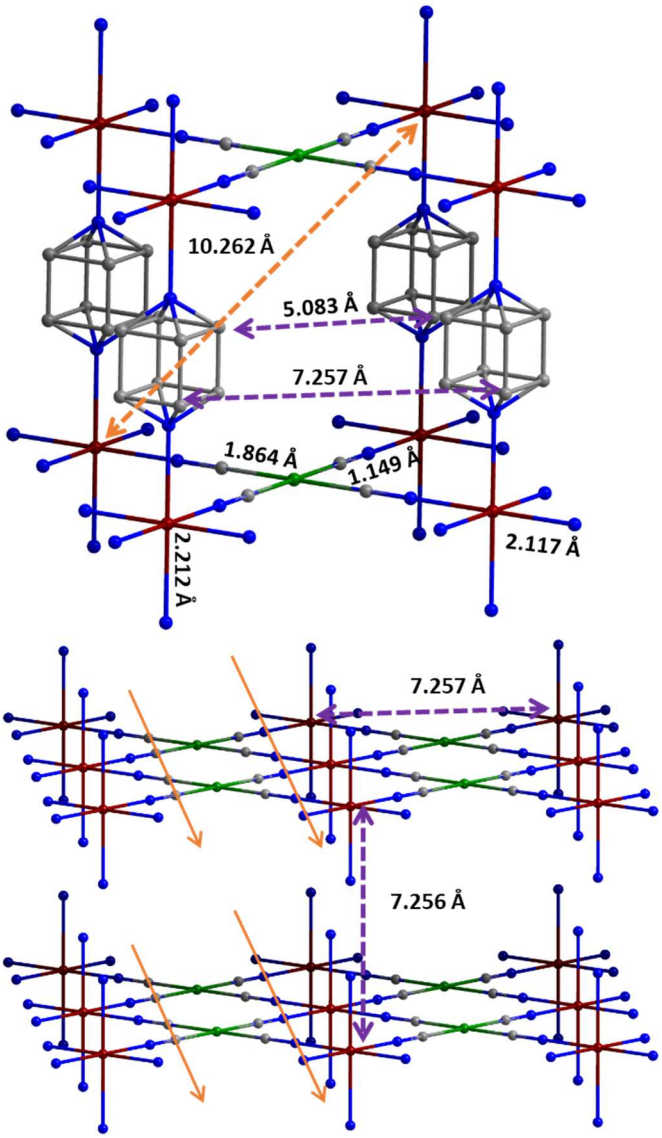

Figure S20: Representation of coordination distances in activated phase of FePzNi structure.

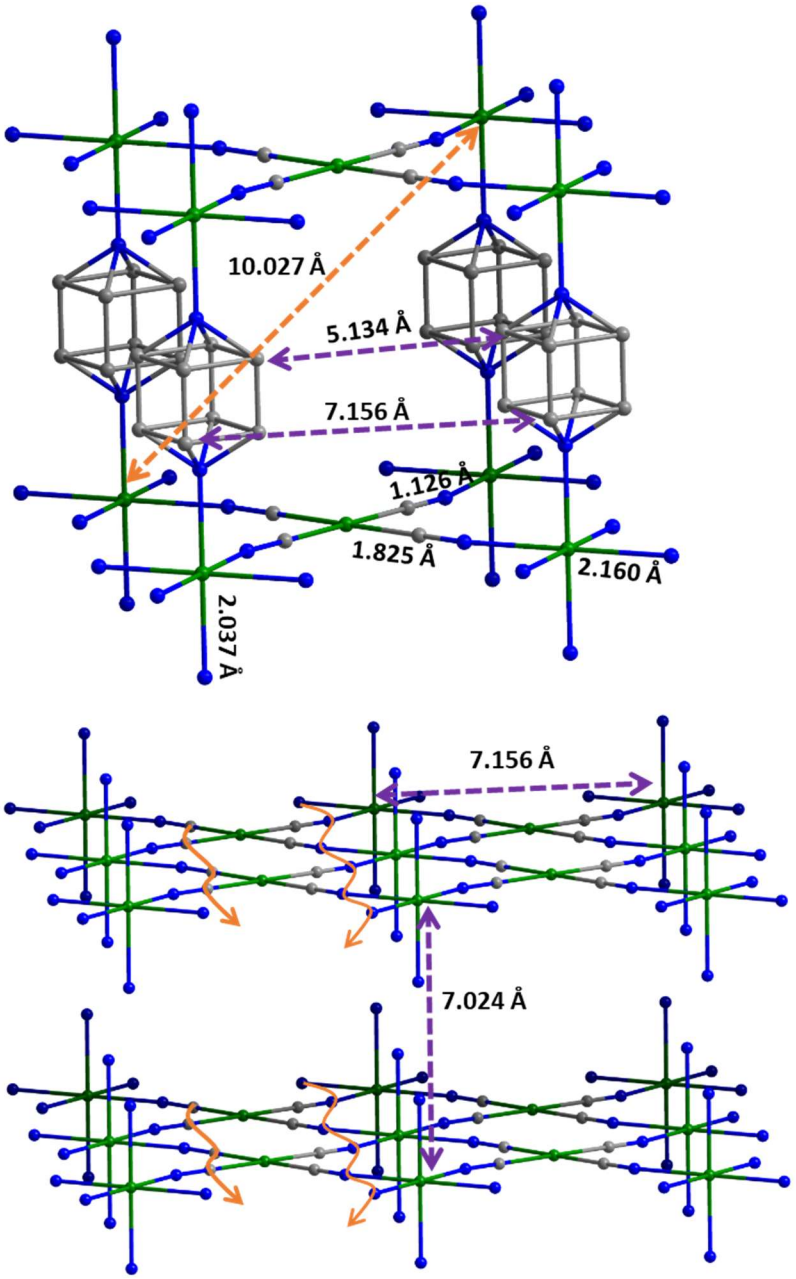

Figure S21: Representation of coordination distances in as synthesized phase of NiPzNi structure. The bond distances in NiPzNi were much shorter compared to both FePzNi and CoPzNi, ($D_{Ni1\cdots Ni3}$ = 10.027(4) Å along diagonal and $D_{Ni1\cdots Ni4}$ = 7.024(4) Å in between the 2D layer); the distance between the octahedral Ni and N atom of the pyrazine ($D_{Ni\cdots N}$ = 2.037(7) Å) and square planar Ni and the C atom of the cyanide ($D_{Ni\cdots C}$ = 1.825(209) Å)).

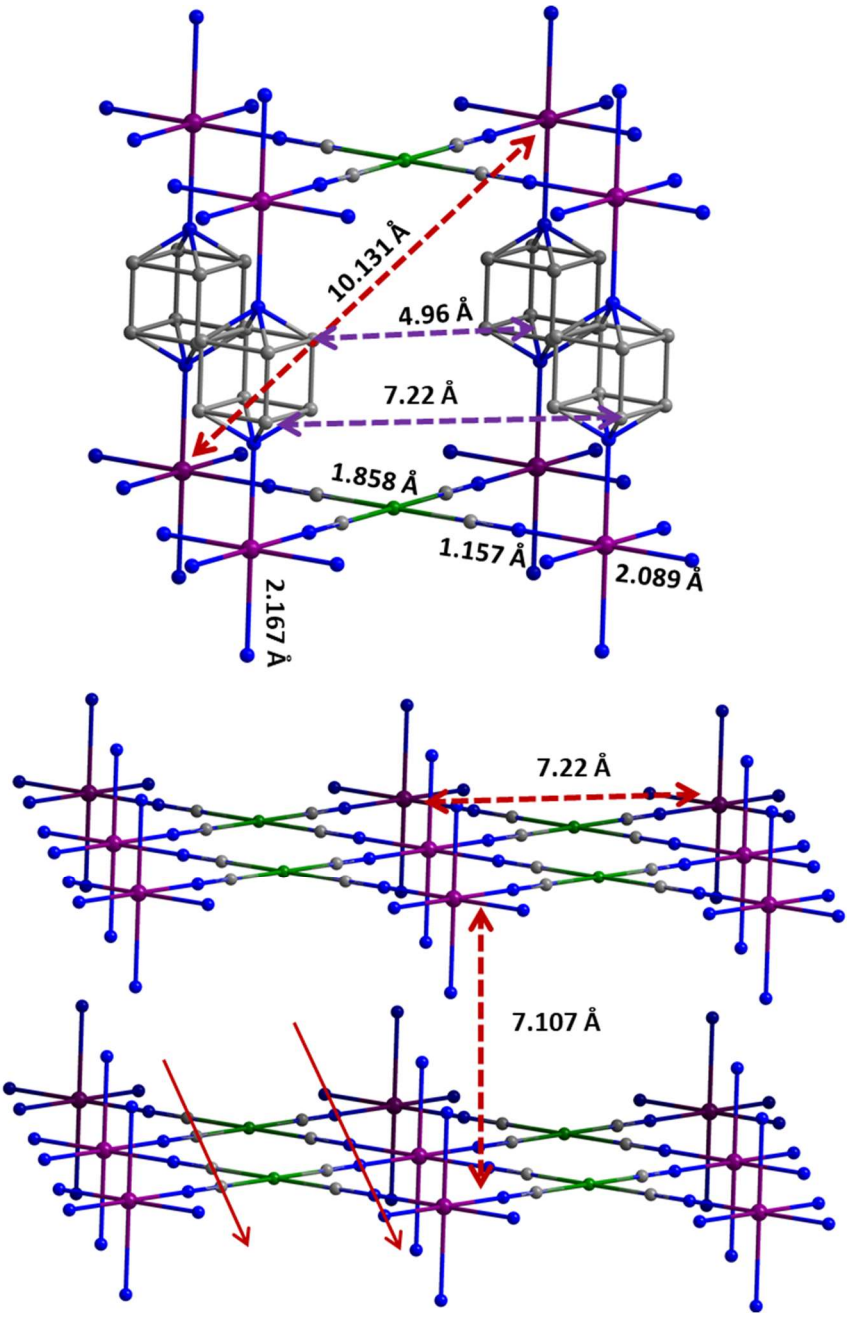

Figure S22: Representation of coordination distances in as synthesized phase of CoPzNi structure. The bond distances in CoPzNi lie between those observed for the FePzNi and NiPzNi structures. For example, the Co···Co distances along the diagonal and between the 2D layer ($D_{Co1\cdots Co3}$ = 10.131(6) Å, and $D_{Co1\cdots Co4}$ = 7.107(6) Å, respectively) (Figure S22 and Table 1), the Co to N (cyanide) distance ($D_{Co\cdots N}$ = 2.089(36) Å), and Co to N (pyrazine) distance ($D_{Co\cdots N}$ = 2.167(64) Å). The square planar Ni center was similar ($D_{Co\cdots C}$ = 1.858(43) Å).

As synthesised

Activated (120°C for 12hrs)

Figure S23: Images of as synthesized (above) and activated (below) samples of FePzNi, CoPzNi and NiPzNi.

Computational Details

The experimentally observed adsorption isotherm of *p*-xylene (***px***) suggests that 0.5 molecules of ***px*** can be adsorbed into one unit cell of three Hofmann-type PCPs (FePzNi, CoPzNi, NiPzNi). To locate the adsorption position ***px***, we carried out canonical Monte-Carlo (MC) simulations,[3] as implemented in RASPA,[4] using Lennard-Jones (LJ) potentials to describe the Van der Waals interaction of ***px*** with PCP framework. The LJ parameters were taken from the standard universal force field (UFF)[5], where the Lorentz-Berthelot mixing rules were used for different atoms. The electrostatic interaction was evaluated with the Ewald summation method, where the DDEC atomic charges[6,7] were used. The MC simulation was carried out by placing 32 ***px*** molecules in a simulation box of 4×4×4 supercell of PCPs. In the MC simulation, the first 2×10^5 cycles were consumed for obtaining equilibration and then 5×10^5 cycles were used for obtaining positions of ***px*** molecules. The final adsorption configuration was used to construct the initial structure for performing geometry optimization with density functional theory (DFT).

The rotation barrier of pyrazine and binding energies of ***px*** into FePzNi, CoPzNi, and NiPzNi were calculated using spin-polarized DFT method with periodic boundary conditions as implemented in the Vienna Ab initio Simulation Package (VASP 5.4.4).[8,9] The Perdew-Burke-Ernzerhof functional[10] with Grimme's semi-empirical "D3" dispersion term[11] (PBE-D3) was employed in these calculations. The plane wave basis sets with an energy cutoff of 850 eV were used to describe valence electrons and the projector-augmented-wave pseudopotentials[12,13] were used to describe core electrons. The criterion of atomic force for geometry optimization was set to be 0.01 eV/Å. One unit cell was used in the calculation of the rotation barrier of pyrazine and a 2×1×1 supercell was used in the calculation of binding energy. The Brillouin zone was sampled by 3×3×3 and 1×3×3 Monkhorst-Pack[14] meshes of *k*-points for one unit cell and 2×1×1 supercell , respectively. Hubbard U correction[15] was applied to the d electrons of Fe, Co, and Ni atoms (U_{eff} = 4.0, 3.3, and 6.4 eV for Fe, Co, and Ni, respectively).[16] In the optimization of the ***px*** adsorption structure, the lattice parameters of PCPs were fixed because the experimental power X-ray diffraction suggested that that little change occurs in the lattices by ***px*** adsorption.

The rotational barrier of the pyrazine ligand was calculated by scanning the potential energy surface against the rotation of the pyrazine ligand along the c axis. The binding energy (*BE*) of ***px*** with PCP was calculated with equation S1;

$$BE = E(\mathrm{PCP}\cdot\mathbf{px}) - E(\mathrm{PCP}) - E(\mathbf{px}) \quad \text{(S1)}$$

where E(PCP·$\mathbf{px}$) is the total energy of PCP **(**PCP **=** FePzNi, CoPzNi, NiPzNi**)** with *1* molecule of ***px*** in equilibrium structure, *E*(PCP) and *E*($\mathbf{px}$) are the total energies of empty PCP and one free ***px*** molecule, respectively.

Table S3. PBE-D3-calculated binding energy, interaction energy between px and PCPs and deformation energy of PCP framework upon px adsorption.

	BE	Eint	Edef
FePzNi	-18.3	-20.8	2.5
CoPzNi	-16.1	-18.8	2.7
NiPzNi	-13.8	-17.0	3.2

Coordinates for optimized adsorption structures of px in three Hofmann-type PCPs.

px@FepzNi

1.00000000000000

14.5223999023000001 0.0000000000000000 0.0000000000000000

0.0000000000000000 7.2401199341000000 0.0000000000000000

0.0000000000000000 0.0000000000000000 7.2791900634999998

Ni Fe N C H

2 2 12 24 18

Direct

0.2492800307416019 0.4996121285171213 0.9998170479944619

0.7493584232768100 0.4997243040121830 0.9998268439521141

0.9990909171265798 0.9996217466023936 0.0233849348391715

0.4997352198380014 0.9998130529531153 0.9763874214797355

0.1028587497042253 0.7902389466989490 0.0383670826650118

0.3956541261527491 0.2088280795153068 0.9609995965955065

0.3927025019318506 0.7987649308211644 0.9962304665695783

0.1059532375068883 0.2005730759454281 0.0039580782477415

0.9951105723061318 0.9948012906280539 0.3311433244178659

0.9943621902504134 0.0065382931585987 0.7142831002448986

0.6034263861280067 0.7913747059877139 0.9739720801775462

0.8952639867709706 0.2078712085102339 0.0258374198173073

0.8931333710658720 0.7962423937344099 0.0178404647532489

0.6055854501910076 0.2032964215315047 0.9818307160445201

0.5051523205532433 0.9933520073657149 0.2853996093633953

0.5045217815655008 0.0049656987494728 0.6685691721099118

0.1594178116885274 0.6749676057220952 0.0337233050363892

0.3391010506446293 0.3241302591491717 0.9657443259791378

0.3373399890567654 0.6815291041336593 0.0058310821527030

0.1612532431815410 0.3178821712459055 0.9940921442516881

0.4263717320594367 0.9963383002513240 0.3809426233323236

0.0731923731183954 0.0035823190719100 0.6188517523518868

0.0735878727542882 0.9910828804033827 0.4279547847437541

0.4260327268078257 0.0087501622853097 0.5718400834671726

0.6600249013697521 0.6767025012173846 0.9832319918437307

0.8386900571031290 0.3225949274138387 0.0164982781057219

0.8372304698577793 0.6800204285696481 0.0112876525752910

0.6615085609724574 0.3194710523591766 0.9883739664374147

0.9158692853663268 0.0033036902519754 0.4265352725945561

0.5837480113373346 0.9966605646149063 0.5730746494279586

0.5841519656983252 0.9954361404179508 0.3819291690727766

0.9154071059251692 0.0045447980768358 0.6176595983817137

0.2209059155944217 0.6395183028337641 0.6153433531881873

0.3142281361141173 0.6176238444014501 0.5754942684578879

0.3460503231807621 0.4788565125211832 0.4585376336266833
0.2794445136888939 0.3604009373258279 0.3844742202621134
0.1861375805051679 0.3822103675969046 0.4243937694831317
0.1543023914975095 0.5210437202170581 0.5412800498739969
0.4471946082166127 0.4612055408044782 0.4169255579676800
0.0531438384015317 0.5387179536927889 0.5826997484776371
0.3627438717618716 0.9875761285069800 0.3024660125189769
0.1367805579220160 0.0124397612624207 0.6974398233367438
0.1374597889652733 0.9774735831749624 0.3507354289493350
0.3621852074159335 0.0222694981254747 0.6491540483553067
0.8525359869017848 0.0082194112665945 0.3463740431880211
0.6471291462009461 0.9918854546178508 0.6531178012949965
0.6479036344594178 0.9947482436225741 0.3029216994532078
0.8516255210949097 0.0053742725462769 0.6965502136093491
0.2001490791765406 0.7488882349629549 0.7088349431570506
0.3640541547472083 0.7070128130947779 0.6423810622626434
0.3001951764596171 0.2511096194442217 0.2909207192376542
0.1363238408900855 0.2926854074491274 0.3576690490823324
0.4841073812099452 0.3952076730755891 0.5316474104682598
0.4596927304666494 0.3808914075411778 0.2917967461388074
0.4786287035999237 0.5976413974071733 0.3966328865911564
0.0405677915666800 0.6190799736502797 0.7077672734119531
0.0163051943434169 0.6046640929716602 0.4678482002261433
0.0217043421146101 0.4022749551666251 0.6029572944035664

px@CopzNi
1.00000000000000
14.3107795714999995 0.0000000000000000 0.0000000000000000
0.0000000000000000 7.1716899871999997 0.0000000000000000
0.0000000000000000 0.0000000000000000 7.1558299065000002
Ni Co N C H
2 2 12 24 18
Direct
0.2499834060954313 0.4999539449056343 0.9999832837096392
0.7499588521043918 0.4999968766072698 0.9999787195244281
0.9988863885190540 0.9998428656763281 0.0345091798392403
0.5009100417649179 0.0001154872193965 0.9650018467487911
0.1020598607529521 0.7941833720646301 0.0439752333711638
0.3979001188168141 0.2058768409235086 0.9558253669255592
0.3969176866577939 0.7985610537427590 0.9840384961316460
0.1031043913350445 0.2011577177067494 0.0153890239373808
0.9957503042185891 0.9949431816526868 0.3396544392252991
0.9945635260288057 0.0051865196260579 0.7282231317787549

0.6029499777017122	0.7951840540292991	0.9634630761422613
0.8970285250606693	0.2050127782913123	0.0359415182571041
0.8961399540407413	0.7971573746763312	0.0304242643481771
0.6037463769145006	0.2027904963431979	0.9693316710428519
0.5049414068896212	0.9941876876550140	0.2713642007101313
0.5037985064106962	0.0051836324075509	0.6598419702330105
0.1595495372611992	0.6780609736513838	0.0382712445188957
0.3404054682148114	0.3219835722829245	0.9616313580561808
0.3403032215525812	0.6818345864718651	0.0005108213803950
0.1596872423170197	0.3179889941028620	0.9992231041149893
0.4248786060135359	0.9961620637761612	0.3674989762842884
0.0746176485832279	0.0034040454739639	0.6320810920399325
0.0752606229336337	0.9909478679981163	0.4378747036224340
0.4242615163266805	0.0090699279515292	0.5616934182440900
0.6600936334291987	0.6792524901349708	0.9763143509968586
0.8398397942399569	0.3208809550695051	0.0233979787437377
0.8391938801040126	0.6806712161695074	0.0194797721589026
0.6606940535988528	0.3192707180875658	0.9804103233793597
0.9151549751316921	0.0023647312578561	0.4358970330326670
0.5843778417320848	0.9973961200729633	0.5635870641912817
0.5850620572628173	0.9968980866172927	0.3692832898638088
0.9144556592399269	0.0024957081401737	0.6302441262824843
0.2214166320500439	0.6421291446033592	0.6166990132919992
0.3156411878158423	0.6192915039413265	0.5726954184581459
0.3469081884911347	0.4780170900805487	0.4543506637104144
0.2785240006861827	0.3578513394634939	0.3830693023840652
0.1842952652614898	0.3806929802758390	0.4270606849397680
0.1530277718219821	0.5219536832746101	0.5454367631831616
0.4492369960984490	0.4602046873038788	0.4093449552951398
0.0507061527561348	0.5397098605074149	0.5905922524417733
0.3606621635358920	0.9860859916105156	0.2868099597775711
0.1388281402787825	0.0131879335864937	0.7127942543488288
0.1399979197603400	0.9773763700236842	0.3591791099797419
0.3595395188233752	0.0230414318430476	0.6404076265584635
0.8510814604119261	0.0072233568197504	0.3537790476404581
0.6484348750032751	0.9925851717111343	0.6457272658864213
0.6497002598004045	0.9971604130483058	0.2887969056622808
0.8497858119091148	0.0018422285171766	0.7106568581097790
0.2015472567883094	0.7536861676631261	0.7112963192757249
0.3668938959621926	0.7095480513028889	0.6381450001629645
0.2983998051071808	0.2462728432421954	0.2885071613902213
0.1330319830904259	0.2904201611816788	0.3616334741190173
0.4873172684371880	0.3923823670881745	0.5245225768319486
0.4611758156414112	0.3804352345001050	0.2810241674124967

0.4810975107209856 0.5980733476396338 0.3894742267340234
0.0388238778714083 0.6196018424692582 0.7188454319678144
0.0125602856935885 0.6073536207606764 0.4754102969614920
0.0189029119863378 0.4018355224365067 0.6107141773830946

px@NipzNi
1.00000000000000
14.2415800094999998 0.0000000000000000 0.0000000000000000
0.0000000000000000 7.1592798233000003 0.0000000000000000
0.0000000000000000 0.0000000000000000 7.0425500870000004
Ni N C H
4 12 24 18
Direct
0.2496683408271565 0.4997327902453250 0.9997694642568007
0.9984816416923152 0.9997402110959328 0.0238052933485093
0.7496945229891665 0.4997692819476356 0.9995175940223362
0.5008738001915916 0.9997054033817605 0.9756430820432698
0.1005912073215214 0.7947836565383497 0.0359119209858818
0.3988045771445243 0.2047910339062327 0.9635325668838632
0.3971114761004344 0.7999486986957649 0.9928017532779165
0.1021946850859763 0.1995654697092419 0.0068410229809359
0.9951505302777193 0.9954662649387060 0.3262880691337173
0.9944141345519384 0.0056492159323582 0.7201423666176723
0.6015600400895238 0.7954800635118815 0.9734666367867604
0.8977160240565283 0.2038563392435009 0.0260128200550653
0.8963479529183687 0.7987680014779954 0.0196682046102268
0.6030788989719298 0.2006950201418078 0.9797022396870716
0.5050419994989710 0.9937752053496780 0.2793627315023883
0.5042516490868891 0.0040117027369604 0.6732195206961435
0.1581819426402475 0.6781265273526103 0.0342057101803732
0.3411638365253893 0.3213773886672655 0.9652563089147250
0.3403254236392570 0.6825025722727958 0.0058373171088064
0.1590065242529022 0.3169601954756658 0.9937923135664875
0.4246672635304733 0.9944553603154631 0.3769501904224839
0.0747822921855175 0.0049506401678698 0.6225480952444258
0.0752258189840305 0.9922800889378038 0.4251826611283036
0.4241968201159949 0.0072073623355493 0.5743196372003183
0.6589335096337763 0.6791041569496343 0.9824629537299430
0.8404013011909726 0.3203364040702468 0.0167853980561716
0.8394242580025448 0.6813927595244564 0.0124954855669444
0.6599842634545041 0.3181271287430150 0.9865961930892411
0.9141565088275314 0.0023257869272157 0.4239726973851106
0.5852565970545598 0.9970906044675232 0.5755735800031658
0.5857454104411914 0.9971621318896453 0.3781745430556072

0.9137002908383423	0.0022868883785137	0.6213862831981203
0.2201108241989473	0.6448852336247128	0.6135666461544318
0.3152575539308842	0.6203075237109914	0.5743512306400120
0.3481514230966809	0.4761341570916926	0.4592253594372835
0.2801916864328717	0.3545909049158524	0.3860365160982724
0.1850631939079150	0.3790761275540078	0.4253141082547032
0.1521632802467323	0.5232815863165428	0.5403929846418123
0.4515364767223105	0.4575201748095736	0.4194926705924971
0.0487756916463908	0.5418429426945579	0.5800416762461040
0.3602311799062434	0.9829874219434132	0.2950694045637405
0.1392301055433762	0.0162334577183927	0.7044353899091220
0.1400506461692288	0.9789144376257042	0.3445925081662153
0.3593608466224936	0.0205370323417782	0.6548838341791168
0.8498250548255797	0.0064780169414078	0.3405072016542761
0.6495641373104419	0.9928070731121252	0.6590991432790148
0.6504817860124348	0.9984580157930196	0.2958400375650854
0.8489929316934379	0.0010539242717087	0.7037928754508584
0.1993283581771124	0.7584076176139547	0.7065850312779034
0.3660615575471056	0.7114783215194720	0.6418094260751843
0.3009787151915617	0.2411894770033314	0.2929370760860053
0.1342853918432212	0.2877994203639247	0.3579973216709078
0.4878683121918428	0.3876223443431002	0.5378459582070931
0.4651862171959422	0.3795832132566588	0.2885548933129201
0.4842398725225436	0.5954900681631017	0.4033933156643030
0.0350519876043833	0.6201602613061610	0.7107201917695676
0.0124372161963322	0.6112914926690891	0.4614188516841509
0.0161511822165181	0.4038581155855070	0.5965779366833104

References

1. Y. Yang, P. Bai and X. Guo, *Ind. Eng. Chem. Res.,* 2017, **56**, 14725-14753.
2. L. Alaerts, C. E. A. Kirschhock, M. Maes, M. A. van der Veen, V. Finsy, A. Depla, J. A. Martens, G. V. Baron, P. A. Jacobs, J. F. M. Denayer and D. E. De Vos, *Angew. Chem. Int. Ed.,* 2007, **46**, 4293-4297.
3. D. Frenkel, and B. Smit, *Understanding Molecular Simulations: From Algorithms to Applications*, Academic Press, San Diego, 2002.
4. D. Dubbeldam, S. Calero, D. E. Ellis and R. Q. Snurr, *Mol. Simul.*, 2016, **42**, 81-101.
5. A. K. Rappe, C. J. Casewit, K. S. Colwell, W. A. Goddard III, and W. M. Skiff, *J. Am. Chem. Soc.*, 1992, **114**, 10024-10035.
6. T. A. Manz and N. Gabaldon Limas, *RSC Adv.*, 2016, **6**, 47771-47801.
7. N. Gabaldon Limas and T. A. Manz, *RSC Adv.*, 2016, **6**, 45727-45747.
8. G. Kresse and J. Furthmüller, *Comput. Mater. Sci.*, 1996, **6**, 15-50.
9. G. Kresse and J. Furthmüller, *Phys. Rev. B*, 1996, **54**, 11169-11186.
10. J. P. Perdew, K. Burke and M. Ernzerhof, *Phys. Rev. Lett.*, 1996, **77**, 3865-3868.
11. S. Grimme, J. Antony, J. Ehrlich and J. Krieg, *J. Chem. Phys.*, 2010, **132**, 154104.
12. P. E., Blöchl, *Phys. Rev. B* 1994, **50**, 17953-17979.
13. G. Kresse and D. Joubert, *Phys. Rev. B,* 1999, **59**, 1758-1775.
14. H. J. Monkhorst and J. D. Pack, *Phys. Rev. B*, 1976, **13**, 5188-5192.
15. S. L. Dudarev, G. A. Botton, S. Y. Savrasov, C. J. Humphreys, and A. P. Sutton, *Phys. Rev. B,* 1998, **57**, 1505-1509.
16. L. Wang, T. Maxisch, and G. Ceder, *Phys. Rev. B,* 2006, **73**, 195107.